



# Aggregation thermodynamics of asphaltenes: Prediction of asphaltene precipitation in petroleum fluids with NRTL-SAC

Md Rashedul Islam, Yifan Hao, Chau-Chyun Chen\*

Department of Chemical Engineering, Texas Tech University, Lubbock, TX, 79409-3121, USA

## ARTICLE INFO

### Article history:

Received 16 January 2020

Received in revised form

11 April 2020

Accepted 14 May 2020

Available online 28 May 2020

### Keywords:

Asphaltene precipitation

Aggregation thermodynamics

NRTL-SAC

Molecule-based characterization

Petroleum fluids

## ABSTRACT

Based on the aggregation thermodynamics established for asphaltene precipitation in binary solvents (Wang et al., *AIChE J.*, 2016, 62 (4), 1254–64; Islam et al., *Fluid Phase Equilibria*, 2018, 473, 255–261), this work extends the aggregation thermodynamics for asphaltene precipitation in blending of heavy oils with light hydrocarbons. In lieu of the commonly accepted pseudocomponents approach for petroleum fluid characterization, the petroleum fluids are characterized in terms of model molecules and their compositions (Chen and Que, U.S. Patent No. 9,934,367 B2, April 3, 2018). Solvent power of the petroleum fluids is further quantified with the conceptual segment-based NRTL-SAC activity coefficient model (Chen and Song, *Ind. Eng. Chem. Res.*, 2004, 43 (26), 8354–62). We show the aggregation thermodynamics with the NRTL-SAC model successfully predicts asphaltene precipitation from crude oils upon blending with normal alkanes.

© 2020 Elsevier B.V. All rights reserved.

## 1. Introduction

Blending of heavy or bituminous oils with lighter crudes is a common practice to reduce viscosity and thereby to aid transportation in crude oil supply chain. However, heavy oils or bitumen with high asphaltene content are vulnerable to asphaltene aggregation upon addition of lighter hydrocarbons. Higher paraffin fraction of lighter hydrocarbon feedstock promotes asphaltene precipitation leading to serious problems, e.g., blockage in the grid line of crude oil supply chain [1]. Therefore, there has been an intense interest in the development of comprehensive thermodynamic models that could predict asphaltene precipitation conditions.

For decades, researchers have been actively pursuing fundamental understanding on the asphaltene precipitation behavior in petroleum fluids with respect to temperature, pressure, and blending of petroleum fluids and crudes. Most of the thermodynamic models for asphaltene precipitation follow the Hansen solubility parameter equation and its variations [2–8]. For example, one of the most recent variations introduced a gravitational term to capture the dispersion of different forms of asphaltenes, i.e., molecules, nanoaggregates, and clusters, along the reservoir depth [9,10]. Apart from these, SAFT-based equation of state (EoS) models

have been introduced to model asphaltene precipitation with respect to temperature and pressure effects [11–13]. However, most of these models describe asphaltene precipitation as a liquid-liquid equilibrium (LLE) phenomenon and they represent crude oils and asphaltenes in terms of “pseudocomponents”. These treatments conflict with the asphaltene structures depicted in the recent Yen-Mullins model [14] which has been well-validated with atomic force microscopy and scanning tunneling microscopy techniques with an atomic resolution [15–17].

Following the Yen-Mullins model, Wang et al. [18] proposed a novel asphaltene aggregation thermodynamics framework which considers the transition of asphaltene molecules to nanoaggregates as asphaltene precipitation. The resulting Gibbs free energy change for this aggregation process can be calculated from the inherent structures of asphaltene molecules and nanoaggregates in the solution. They showed the aggregation thermodynamics qualitatively predicts asphaltene precipitation from binary mixtures of organic solvents using UNiversal Functional group Activity Coefficient (UNIFAC), CONductor like Screening MODEls Segment Activity Coefficient (COSMO-SAC), and NonRandom Two-Liquid Segment Activity Coefficient (NRTL-SAC) models [18–26]. Among these models, NRTL-SAC is the model of choice due to its capability to correlate and predict precipitation behavior of diverse asphaltene molecules with a minimal number of structural parameters [25]. Specifically, NRTL-SAC treats all molecules with four distinctive conceptual segments: hydrophobic, polar attractive, polar

\* Corresponding author.

E-mail address: [chauchyun.chen@ttu.edu](mailto:chauchyun.chen@ttu.edu) (C.-C. Chen).

repulsive, and hydrophilic. The numbers of conceptual segments for asphaltenes and nanoaggregates can be identified from experimental asphaltene precipitation data. In contrast, UNIFAC and COSMO-SAC must pre-assume specific molecular structures for the asphaltene molecules.

This work takes on the challenge of extending the aggregation thermodynamics to the prediction of asphaltene precipitation from blending of crude oils with hydrocarbon diluents. To illustrate the approach, we perform thermodynamic modeling of asphaltene precipitation in three heavy oils: Athabasca, Cold Lake, and Peace River. In lieu of the commonly accepted pseudocomponents approach for petroleum fluid characterization, a novel “model molecule-based characterization” (MC) technique [27] is used. Designed to accurately predict physical and chemical properties of blends of petroleum fluids, the MC technique determines the molar compositions of petroleum fluids and their blends in terms of a collective set of pre-defined model hydrocarbon molecules from regression of measurable petroleum properties such as distillation curve, density, viscosity, and hydrocarbon contents, which are readily available in typical petroleum assays. These model hydrocarbon molecules and their compositions are then grouped into asphaltenes and maltenes, i.e., de-asphalted crude oil. Subsequently, the NRTL-SAC conceptual segments of asphaltenes, nanoaggregates, and maltenes are estimated from available asphaltene precipitation data. Lastly, NRTL-SAC is used to predict asphaltene precipitation in the blends of crude oils and hydrocarbon diluents and the alkane volume fraction at the onset of asphaltene precipitation.

## 2. Asphaltene precipitation data

There is a plethora of asphaltene precipitation measurements in the literatures [2–8,28]. Over several decades, researchers have conducted experimental asphaltene stability studies to examine the effects of change in composition, pressure, and temperature. Briefly summarized here are the composition-induced asphaltene solubility and precipitation measurements.

Mannistu et al. reported asphaltene solubility in 15 binary solvents [4]. Based on asphaltene solubility, solvents were categorized as good and poor. Good solvent list included toluene, *t*-butyl benzene, nitrobenzene, dichloromethane, cyclohexane, and decalin. Poor solvents were *n*-pentane, *n*-hexane, *n*-heptane, *n*-octane, *n*-decane, *i*-pentane, *i*-octane, 1-hexene, acetone, and methanol. Binary mixtures were formulated by pairing toluene with poor solvents and pairing *n*-hexane with good solvents. Asphaltenes were extracted from Athabasca bitumen upon mixing with *n*-heptane at a 40:1 vol ratio of *n*-heptane and bitumen. The extracted asphaltenes were purified by subsequent filtration and drying. Solid asphaltenes at a concentration of 8.8 kg/m<sup>3</sup> were added to a binary solvent of known ratio for solubility measurements. The mass ratio of insoluble asphaltenes and total asphaltenes were measured at different volume ratio of the constituent solvents. Table 1 summarizes the asphaltene solubility measurements [4].

Crude oils were also diluted with *n*-alkanes for precipitation measurements [5–8]. Mixtures of crude oils and *n*-heptane of known volume ratio were left to settle for a prolonged time. Precipitated asphaltenes were collected after decantation of supernatant. Recovered asphaltenes were further washed with *n*-heptane and dried completely before measurement. Asphaltene precipitation yields were reported as the mass ratio of precipitated asphaltenes over total crude oil. Table 2 showcases asphaltene precipitation from three different crude oils: Athabasca [8], Peace River [8], and Cold Lake [5].

The precipitation onset point is another important measurement to assess precipitation from crude oils. The minimum volume of *n*-alkane required for the first appearance of asphaltene

precipitation from a known volume of crude oil is defined as the onset point of precipitation. Wiehe et al. measured the onset point of crude oils against *n*-alkanes ranging from *n*-pentane to *n*-hexadecane [28]. See Table 3. It has been observed that the volume of *n*-alkanes required to reach the onset point increases with the carbon number and reaches a maximum in the range of *n*-C<sub>8</sub> to *n*-C<sub>10</sub> [28,29]. These onset points were measured by incremental addition of *n*-alkanes to crude oils. After each addition, appearance of precipitation is detected under optical microscopy at 100× magnification.

## 3. Thermodynamic models

The inception of asphaltene precipitation follows aggregation of asphaltene molecules to nanoaggregates. Modeling the change in Gibbs free energy for this transition leads to development of the aggregation thermodynamics model for asphaltene precipitation [18,21,25]. To properly address the diverse nature of molecular species present in crude oils, the conceptual segment concept of the NRTL-SAC activity coefficient model offers a simple and practical approach to fully account for the change in Gibbs free energy derived from the complex molecular interactions associated with the aggregation process [18,21,25].

### 3.1. Aggregation thermodynamics

The aggregation process of asphaltene is viewed as two steps: 1) asphaltene molecules stack together and assume highly ordered structure, i.e., nanocrystals, and 2) nanocrystals re-dissolve into the solution by relaxing on their rigid structure and forming nanoaggregates. See Fig. 1 [21]. These phase transitions can be quantified to estimate the change in Gibbs free energy for each step.

$$\frac{\Delta G_{M \rightarrow A}}{RT} = \frac{\Delta G_{M \rightarrow C}}{RT} + \frac{\Delta G_{C \rightarrow A}}{RT} \quad (1)$$

where  $\Delta G$  is the change of Gibbs free energy;  $R$  is the gas constant;  $T$  is the system temperature. Subscripts  $M$ ,  $C$ , and  $A$  denote asphaltene molecules, nanocrystals, and nanoaggregates in solution, respectively.

The change in Gibbs free energy for the crystallization process,  $\Delta G_{M \rightarrow C}$ , can be further expressed with the solubility constant,  $K_s$ :

$$\frac{\Delta G_{M \rightarrow C}}{RT} = -\ln K_s = -(\ln x_i^{sat} + \ln \gamma_i^{sat}) \quad (2)$$

where  $x_i^{sat}$  and  $\gamma_i^{sat}$  are the solubility and the activity coefficient of asphaltene molecules at saturation, respectively.

The change in Gibbs free energy for the dissolution of nanocrystals to nanoaggregates,  $\Delta G_{C \rightarrow A}$ , is approximated with the infinite dilution activity coefficient of nanoaggregates in the solution.

$$\frac{\Delta G_{C \rightarrow A}}{RT} \cong \ln \gamma_{nano}^{\infty} \quad (3)$$

here the infinite dilution activity coefficient,  $\gamma_{nano}^{\infty}$ , is attributed to the solvent-nanoaggregate interaction. Since only the alkyl side chains of nanoaggregates are exposed in the solution,  $\gamma_{nano}^{\infty}$  should be dominated by the interaction between the solvent and the alkyl side chains.

Summing up Eqs. (1)–(3) and expressing  $\Delta G_{M \rightarrow A}$  with a nanoaggregate formation constant,  $K_f^{agg}$ , the expression for aggregation thermodynamics is derived as follows:

**Table 1**  
Asphaltenes solubility measurements in organic solvents [4].

Good solvent	Poor solvent	Volume fraction of good solvent in binary system	Number of data points
toluene	<i>n</i> -pentane	0.073~0.60	11
toluene	<i>n</i> -hexane	0.072~0.48	14
toluene	<i>n</i> -heptane	0.072~0.39	12
toluene	<i>n</i> -octane	0.070~0.48	11
toluene	<i>n</i> -decane	0.070~0.48	11
toluene	<i>i</i> -pentane	0.073~0.60	7
toluene	<i>i</i> -octane	0.075~0.50	11
toluene	acetone	0.197~0.80	7
toluene	ethanol	0.196~0.90	7
toluene	1-hexene	0.071~0.50	6
nitrobenzene	<i>n</i> -hexane	0.099~0.50	10
<i>t</i> -butyl benzene	<i>n</i> -hexane	0.160~0.85	9
cyclohexane	<i>n</i> -hexane	0.165~1.00	24
decalin	<i>n</i> -hexane	0.167~0.70	7
dichloromethane	<i>n</i> -hexane	0.050~0.50	9

**Table 2**  
Asphaltenes precipitation measurements from crude oils.

Athabasca [8]		Cold Lake [5]		Peace River [8]	
<i>n</i> -C <sub>7</sub> mass frac.	Asphaltene precipitation yield	<i>n</i> -C <sub>7</sub> mass frac.	Asphaltene precipitation yield	<i>n</i> -C <sub>7</sub> mass frac.	Asphaltene precipitation yield
0.50	0.003	0.55	0.004	0.58	0.033
0.58	0.006	0.63	0.025	0.67	0.075
0.67	0.027	0.63	0.023	0.73	0.083
0.67	0.035	0.70	0.061	0.77	0.096
0.73	0.063	0.71	0.056	0.87	0.113
0.77	0.071	0.77	0.083	0.93	0.120
0.77	0.075	0.77	0.080		
0.87	0.104	0.84	0.097		
0.88	0.104	0.89	0.105		
0.93	0.113	0.93	0.110		
0.93	0.119				

$$\frac{\Delta G_{M \rightarrow A}}{RT} = -\ln K_I^{agg} = -\left(\ln x_I^{agg} + \ln \frac{\gamma_I^{agg}}{\gamma_{nano}^{\infty}}\right) \quad (4)$$

where  $x_I^{agg}$  and  $\gamma_I^{agg}$  are the mole fraction and the activity coefficient of asphaltene molecules in the solution. In this work,  $\gamma_I^{agg}$  and  $\gamma_{nano}^{\infty}$  are calculated by a modified NRTL-SAC activity coefficient model [25].

### 3.2. NRTL-SAC model

According to the NRTL-SAC model [26], the activity coefficient for component *I* in the solution is calculated in two parts:

$$\ln \gamma_I = \ln \gamma_I^C + \ln \gamma_I^R \quad (5)$$

here  $\gamma_I^C$  is the activity coefficient from the combinatorial contribution, and  $\gamma_I^R$  is the activity coefficient from the residual contribution. Following our earlier work with NRTL-SAC [25], we calculate  $\gamma_I^C$  with a modified Staverman-Guggenheim (SG') expression to account for the size and shape differences of molecules in solution:

$$\ln \gamma_I^C = \ln \gamma_I^{SG'} = 1 - \frac{\phi'_I}{x_I} + \ln \frac{\phi'_I}{x_I} - \frac{1}{2} Z q'_I \left( 1 - \frac{\phi'_I}{\theta'_I} + \ln \frac{\phi'_I}{\theta'_I} \right) \quad (6)$$

$$\phi'_I = \frac{r'_I x_I}{\sum_j r'_j x_j} \quad \text{and} \quad \theta'_I = \frac{q'_I x_I}{\sum_j q'_j x_j} \quad (7)$$

**Table 3**  
Volume fraction of *n*-alkanes at the onset of asphaltene precipitation [28].

Alkanes	Athabasca	Cold Lake
<i>n</i> -C <sub>5</sub>	0.650	0.587
<i>n</i> -C <sub>6</sub>	0.669	0.608
<i>n</i> -C <sub>7</sub>	0.671	0.623
<i>n</i> -C <sub>8</sub>	0.669	0.636
<i>n</i> -C <sub>9</sub>	0.673	0.649
<i>n</i> -C <sub>10</sub>	0.669	0.636
<i>n</i> -C <sub>11</sub>	0.669	0.623
<i>n</i> -C <sub>12</sub>	0.669	0.608
<i>n</i> -C <sub>13</sub>	0.660	0.592
<i>n</i> -C <sub>14</sub>	0.645	0.574
<i>n</i> -C <sub>15</sub>	0.630	0.556
<i>n</i> -C <sub>16</sub>	0.618	0.550

$$r'_I = r_I^p \quad \text{and} \quad q'_I = q_I^p \quad (8)$$

here,  $\phi'_I$ ,  $\theta'_I$ ,  $r'_I$ , and  $q'_I$  are the modified volume fraction, surface area fraction, normalized volume, and normalized surface area parameters, respectively. *Z* is the coordination number, which is taken as 10 as in the original Staverman-Guggenheim model [30]. The exponent parameter *p* is taken as 2/3, identified by comparing with experimental infinite dilution activity coefficient of alkane mixtures [21]. The volume and surface area of molecules are calculated from the van der Waals radii of atoms using the Bondi's method [31]. The van der Waals volume and surface area of molecule are further normalized by the van der Waals volume and surface area of a standard segment to find  $r_I$  and  $q_I$  respectively as outlined by Abrams and Prausnitz [30].

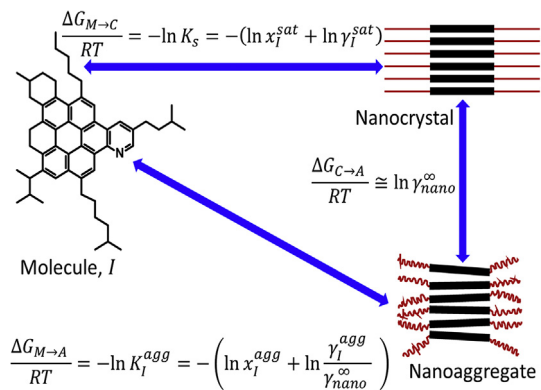


Fig. 1. Transition of asphaltene molecule to nanoaggregate [21].

The residual term  $\gamma_I^R$  is calculated from the local composition ( $lc$ ) interaction contribution  $\gamma_I^{lc}$  of Polymer NRTL model [32]:

$$\ln \gamma_I^R = \ln \gamma_I^{lc} = \sum_m r_{m,I}^s \left[ \ln \Gamma_m^{lc} - \ln \Gamma_{m,I}^{lc} \right] \quad \text{where, } m \in [X, Y^-, Y^+, Z] \quad (9)$$

where  $m$  is the segment species index,  $\Gamma_m^{lc}$  and  $\Gamma_{m,I}^{lc}$  are the activity coefficient of segment species  $m$  in solution and in component  $I$  respectively. The modified NRTL-SAC model suggests 4 conceptual segments to represent major molecular characteristics: hydrophobic ( $X$ ), polar attractive ( $Y^-$ ), polar repulsive ( $Y^+$ ), and hydrophilic ( $Z$ ). With the temperature-dependent interaction parameters between segments available in the literature [25], segment numbers of different components can be determined from their phase equilibrium data, e.g., vapor-liquid equilibrium (VLE), liquid-liquid equilibrium (LLE), and solid-liquid equilibrium (SLE).

The modeling procedures for asphaltene precipitation in crude oils are elaborated in Fig. 2. A molecule-based characterization technique is first applied to represent the crude oil with a set of pre-defined model hydrocarbon molecules and the molar distribution of the model molecules. Based on their molecular structures, the molecules are then grouped into asphaltenes and maltenes, and subsequently the average molecular weight,  $\overline{MW}$ , and average structural parameters,  $\bar{r}_I$  and  $\bar{q}_I$ , are computed for asphaltenes and maltenes. The conceptual segment numbers of NRTL-SAC model are further identified from pertinent asphaltene precipitation data. Finally, the asphaltene precipitation behavior can be predicted for the crude oil.

#### 4. Molecule-based characterization of petroleum fluids

Molecule-based characterization (MC) of petroleum fluids is a novel approach for finding representative molar compositions of petroleum fluids from crude oil assay data [27]. Briefly, MC generates a pool of pre-defined model hydrocarbon molecules with their relative amounts, i.e., mole fractions, to represent a given crude oil

or petroleum fraction. These molecules and their compositions are generated from distribution functions of sets of repeat units, or structural segments, designed to represent typical classes of hydrocarbon molecules present in petroleum fluids. The petroleum properties of these molecules and their mixtures are then calculated from segment-based thermodynamic models and correlations. The distribution functions and the corresponding molecular compositions are adjusted until the calculated petroleum properties satisfactorily mimic those reported in crude oil assay for the crude oil. While details of the MC methodology are available in the literature [27], key features of the MC methodology are summarized here.

Crude oils contain virtually infinite number of different hydrocarbon molecules. As a minimum, MC identifies three main classes of hydrocarbon molecules in crude oil: paraffins (P), naphthenes (N), and aromatics (A). Specifically, paraffinic molecules contain linear and branched alkanes; naphthenic molecules contain cyclic alkanes and fused naphthenic rings with alkyl side chains; aromatic molecules contain single or polycyclic aromatic rings with alkyl side chains and naphthenic rings. Additional subclasses of hydrocarbon molecules may be incorporated. For example, hydrocarbon molecules with hetero atoms, such as O, N, and S, forms additional subclasses. Sulfides, mercaptans, naphthenic sulfides, and thiophenes are sulfur-based subclasses. Carbazoles and quinolines are nitrogen-based subclasses. Phenols, aromatic acids, and naphthenic acids are oxygen-based subclasses.

Thus, MC represents crude oils as mixtures of the molecules from the hydrocarbon classes and subclasses. The molecules from each class or subclass are further represented by a set of repeat units, or structural segments, that make up the molecules. For example, Table 4 shows the structural segments of the hydrocarbon classes: P, N, and A, respectively. Additional structural segments are added to these segments to generate molecules for the subclasses.

The occurrence of segments appearing in each molecule is controlled by use of probability distribution functions (pdf). The probabilities of each segment in a molecule or compound lead to the calculation of molar concentration of that molecule. For instance, if an *iso*-paraffin molecule contains  $l$  number of  $-CH_2-$  segment,  $m$  number of  $>CH-$  segment, and  $n$  number of  $>C<$  segment, the mole fraction ( $y_{l,m,n}^P$ ) of the molecule in the whole crude is calculated as the product of the segment probabilities and the mole fraction of P class,  $y_P$ . See Eq. (10). A three-parameter gamma distribution function is used to define the occurrence of segments. See Eq. (11). The probability of  $n$ -th occurrence of a segment,  $p(n)$ , depends on the shape factor,  $\alpha$ , the scale parameter,  $\beta$ , and the starting point of distribution,  $L$ . With this segment approach, all the molecules of different classes and subclasses are generated *a priori* and the molar compositions are calculated from the probabilities of each molecule.

$$y_{l,m,n}^P = y_P \times p_P^{-CH_2-}(l) \times p_P^{>CH-}(m) \times p_P^{>C<}(n) \quad (10)$$

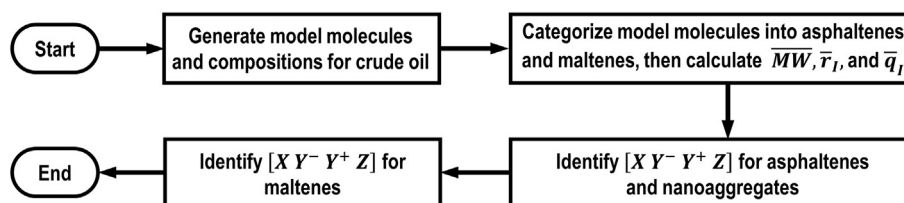


Fig. 2. Flowchart of overall modeling procedure of asphaltene precipitation from crude oil.

**Table 4**  
Hydrocarbon segments [27].

Segments	Occurrence range
	0~60 <sup>a</sup> 0~48 <sup>b</sup> 0~48 <sup>c</sup> 0~3
	0~2
	1
	1
	1
	0~6
	1
	0~6

<sup>a</sup> Paraffins.  
<sup>b</sup> Naphthenes.  
<sup>c</sup> Aromatics.

$$p(n) = \frac{(n-L)^{\alpha-1} e^{-\frac{n-L}{\beta}}}{\beta^{\alpha} \Gamma(\alpha)} \quad (11)$$

The segment approach is also extensively used in the calculation of petroleum properties such as boiling point, density, and viscosity. For example, segment-based PC-SAFT EoS [33] is employed to calculate boiling points and densities of the compounds. The PC-SAFT model parameters for the segments are identified from regression of experimental vapor pressure, liquid density, and heat capacity of hundreds of pure compounds that contain the segments.

Upon generation of the model molecules and the molar compositions, the bulk assay properties, both physical and chemical, of the whole crude oil and their distillation cuts can be estimated. The gamma distribution function parameters can then be adjusted to minimize the residual root-mean-square error (RRMSE) of the estimated and the measured properties reported in the crude assay. The entire MC process is depicted in Fig. 3. RRMSE is described in Eq. (12).

$$RRMSE = \sqrt{\frac{\sum_i^k \sum_j^m \left( \frac{\hat{z}_{ij} - z_{ij}}{\sigma_{ij}} \right)^2}{km - n}} \quad (12)$$

where  $\hat{z}$  and  $z$  are the estimated and the measured properties respectively;  $\sigma$  is the standard deviation of the property measurement;  $i$  is the property type index;  $k$  is the total number of the property types;  $j$  is the data point index;  $m$  is the total number of data points for a particular property type;  $n$  is the total number of adjustable parameters.

In summary, MC offers a systematic methodology that optimizes the model molecules and their molar compositions to best represent a petroleum fluid expressed with its crude oil assay. The MC calculations in this study are carried out with the process simulation software Aspen HYSYS® [34].

### 5. Three crude oils and their molecular compositions from MC

The MC method is applied to determine the molecular make-up of Athabasca bitumen, Cold Lake bitumen, and Peace River bitumen. The assays for these three crude oils have been reported by Alberta Department of Energy (DoE) [35] for six cuts: naphtha, distillate, light gas oil (LGO), heavy gas oil (HGO), vacuum gas oil (VGO), and vacuum residue (VR). The temperature ranges for these cuts are initial boiling point (IBP) – 266 °C, 266–343 °C, 343–399 °C, 399–454 °C, 454–527 °C, and 527 °C – final boiling point (FBP), respectively. The assay includes a wide spectrum of physical, chemical, and transport properties of the crude oils and their cuts as shown in Table 5 for Athabasca bitumen. With these assay data, the MC of Athabasca bitumen is performed. Fig. 4 plots the molecule distributions in terms of PNA classes at different distillation temperatures, and it shows the calculated PNA content of naphtha and distillate cuts are in good agreement with their measured values. It also shows that Athabasca bitumen contains mostly naphthenic and aromatic molecules, with aromatics dominating the heavier (higher boiling temperature) cuts. The heavy aromatic components contain significant amount of asphaltenes, which is supported by the measured asphaltene content, as high as 33 wt%, in the vacuum residue cut [35].

With the optimized molecular composition for Athabasca bitumen, the calculated assay properties satisfactorily match the reported assay data. As an illustration, Fig. 5 shows the calculated distillation curve, density, viscosity, and asphaltene content of Athabasca bitumen. Specifically, the calculated cumulative distillation yields at different temperatures are shown in Fig. 5a. The calculations agree well with the reported cut yields. Fig. 5b and c shows the calculated liquid density and viscosity respectively for products

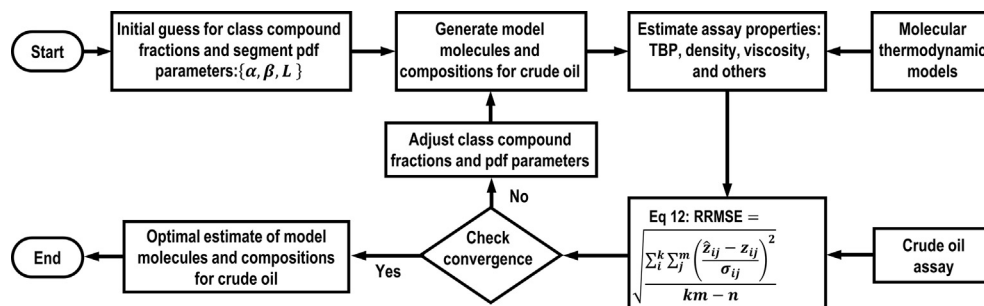
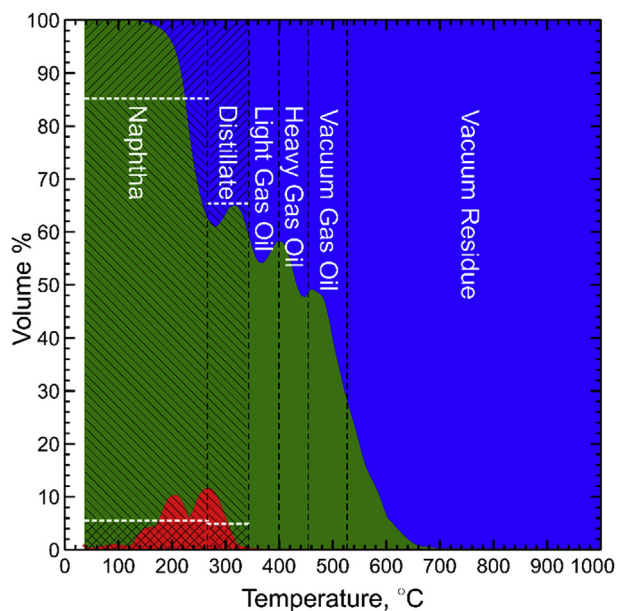


Fig. 3. Molecule-based characterization methodology [27].

**Table 5**  
Assay properties of Athabasca bitumen and its cuts [35].

	Whole crude	Naphtha	Distillate	LGO	HGO	VGO	VR
Boiling range (°C)		IBP –266	266–343	343–399	399–454	454–527	527 – FBP
Yield (wt.%)		1.81	7.93	9.51	9.03	15.71	56.01
Yield (vol.%)		2.10	8.87	10.22	9.38	16.15	53.28
API gravity	8.10	31.33	25.09	18.79	14.00	12.41	1.67
TAN (mg KOH/g)	2.33	0.50	1.27	3.12	3.10	3.48	0.96
Aniline point (°C)		56	54	121	50	56	
Cloud point (°C)		–34	–35	–41			
Pour point (°C)		–65	–59	–33	–10	12	
Softening point (°C)							77
Smoke point, (mm)		21					
Cetane index			39				
K factor		11.30	11.29	11.24	11.17	11.29	
Ash content (wt.%)	0.20						
MCR (wt.%)	14			0.01	0.03	0.49	25
Nitrogen (ppm)	4431	32	142	608	1385	2537	6823
Sulfur (wt.%)	5	0.95	1.79	2.9	3.6	3.9	6.6
Asphaltenes (wt.%)							
C <sub>5</sub> insoluble	19						33
C <sub>7</sub> insoluble	11						20
Metal content (ppm)							
Iron	8						15
Nickel	85						153
Vanadium	222						399
PNA content (vol.%)							
P		5.5	4.9				
N		79.7	60.4				
A		14.8	34.7				
Viscosity (cSt.)							
30 °C		3	9				
40 °C		2					
50 °C		2	5	19	97	594	
70 °C	1756		3	9	32	134	
80 °C	871						
90 °C	472			5	14	45	402 × 10 <sup>3</sup>
100 °C							131 × 10 <sup>3</sup>
110 °C							48 × 10 <sup>3</sup>



**Fig. 4.** Paraffins (red), naphthenes (green), and aromatics (blue) distribution along boiling point temperatures. Black dashed lines represent distillation cuts. White dashed lines in the hatched region represent the reported PNA content in Naphtha and Distillate [35]. P (⊗), N (⊘), and A (⊙).

of different true boiling point (TBP). Fig. 5d shows the calculated asphaltene content in different TBPs up to 700 °C. Athabasca crude assay [35] reports asphaltene content in vacuum residue (TBP above 527 °C) is 33.48 wt% (dashed line in Fig. 5d) and in the whole crude is 18.9 wt%, in line with the MC calculations. Other properties like total acid number (TAN), aniline point, cloud point, pour point, softening point, smoke point, cetane index, Watson K factor, ash content, asphaltene content, micro carbon residue (MCR), nitrogen content, sulfur content, and metal content as listed in Table 5 are all well fitted simultaneously. Overall, although the optimized molecular composition for Athabasca bitumen is by no means unique, MC generates a molecular composition in terms of a selected set of model molecules that is a good representation of the crude oil with the reported assay data.

MC is also implemented for Peace River bitumen and Cold Lake bitumen. Table 6 reports mass percentages of molecules in various classes and subclasses for the three crude oils. Note that paraffins, naphthenes, aromatics, thiophenes, and quinolines contribute to over 98 wt% of each crude oil. Therefore, for simplification purpose, the other three subclasses of molecules (carbazoles, naphthenic acids, and aromatic acids) are excluded from the subsequent asphaltene precipitation studies. The identified gamma distribution function parameters are reported in Table 7. The location parameter  $L$  is taken as  $-1$  for all gamma distributions.

## 6. Aggregation thermodynamics for crude oils

Per Yen-Mullins model [14], asphaltene molecules are moderate-sized polycyclic hydrocarbons with peripheral alkane

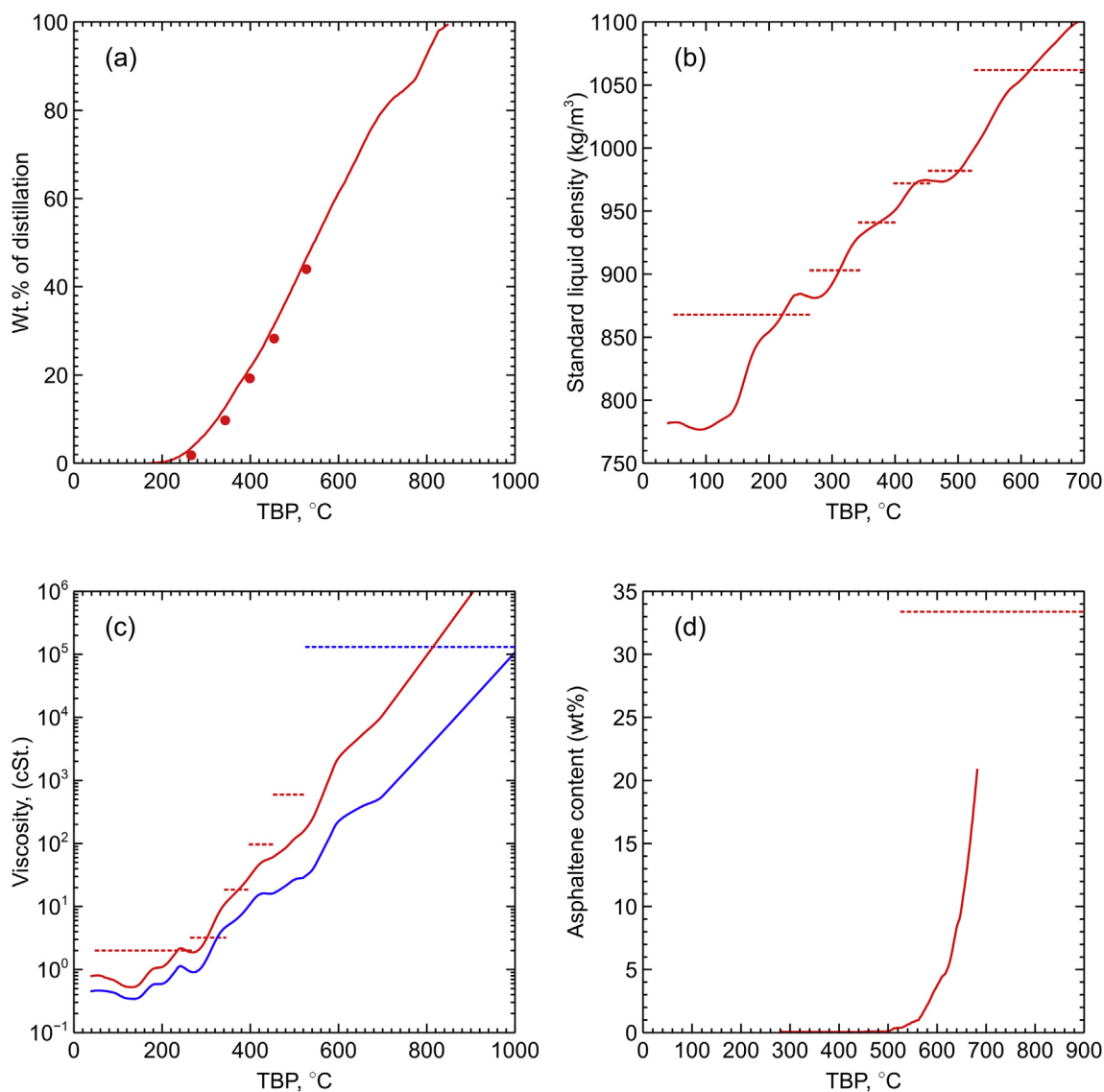


**Fig. 5.** Calculated properties (solid lines) of Athabasca bitumen compared to assay data [35] (solid circles and dashed lines): (a) distillation yield, (b) density, (c) viscosity at 50 °C (red) and 100 °C (blue), and (d) asphaltene content in different TBP products.

**Table 6**  
Mass distributions of molecules in various classes and subclasses.

	Athabasca (wt.%)	Peace River (wt.%)	Cold Lake (wt.%)
Paraffins	0.46	1.54	1.79
Naphthenes	26.03	24.39	28.99
Aromatics	38.78	32.01	36.93
Thiophenes	25.90	30.51	23.28
Quinolines	7.15	10.39	7.15
Carbazoles <sup>d</sup>	0.41	0.24	1.05
Naphthenic acids <sup>d</sup>	0.83	0.56	0.62
Aromatic acids <sup>d</sup>	0.44	0.36	0.20
<b>Total</b>	<b>100</b>	<b>100</b>	<b>100</b>

<sup>d</sup> Model molecules not considered as asphaltenes or maltenes.

substituents. Their molecular weights are in the range between 500 and 1000 Da. Heteroatoms such as S, N, and O may also be present. Accordingly, we relate asphaltenes with the heavy ends of aromatics, thiophenes and quinolines. In these three classes, asphaltenes are those molecules with more than 4 fused aromatic rings

and with molecular weight larger than 480 g/mol, 450 g/mol, and 450 g/mol for Athabasca, Peace River, and Cold Lake bitumen, respectively. With such cutoff criteria, the asphaltene weight percentages are in line with the reported asphaltene contents [35] (parenthesized numbers in Table 8). The molar composition of each group, i.e., asphaltenes and maltenes, is then normalized to unity. From the chemical structure of each component resulted from the molecular characterization, the volume and surface area parameters are computed. The molar average molecular weight ( $\overline{MW}$ ) and average molecular structural parameters ( $\overline{r}_l$  and  $\overline{q}_l$ ) are reported in Table 8. For all the three heavy oil samples, asphaltenes molecular structural parameters come out very close. Therefore, same proxy molecule for nanoaggregates should be acceptable in calculating asphaltene precipitations from the samples. The compositions and parameters reported in Table 8 are assumed in the subsequent quantification of conceptual segment numbers for asphaltenes, nanoaggregates, and maltenes, and the calculations for asphaltene precipitation.

**Table 7**  
Gamma distribution parameters for segments.

Class	Segments	Athabasca		Peace River		Cold Lake	
		$\beta$	$\alpha$	$\beta$	$\alpha$	$\beta$	$\alpha$
Paraffins		0.01	1.66	0.01	1.66	0.01	1.66
		0.04	100	0.04	100	0.04	100
		18.97	5.26	129	1.00	0.05	72.27
Naphthenes		0.97	3.71	11.10	0.01	3.45	0.85
		5.55	2.05	14.50	0.54	7.22	1.35
Aromatics		1000	1.27	263.10	1.07	961.30	0.96
		0.01	1.00	0.01	1.00	0.01	1.00
		0.19	53.93	0.07	100	0.56	15.92
Thiophenes		1.77	1.61	5.22	0.41	3.18	0.75
		0.01	0.01	0.02	0.04	0.01	0.12
		1.63	10.49	1.59	8.64	2.01	7.67
Quinolines		0.74	6.28	0.96	2.86	0.63	5.04
		1000	61.09	1000	61.00	996	50.97
		9.69	1.93	42.40	2.84	24.44	1.85

**Table 8**  
Calculated properties for maltenes and asphaltenes.

	Athabasca		Peace River		Cold Lake	
	Maltenes	Asphaltenes	Maltenes	Asphaltenes	Maltenes	Asphaltenes
Wt.%	81.04	18.96 (18.74)	84.74	15.26 (16.38)	81.30	18.70 (17.09)
$\overline{MW}$	357	556	309	552	313	549
$\bar{r}_l$	15.30	22.59	13.23	22.40	13.49	22.47
$\bar{q}_l$	12.57	15.60	9.53	15.51	9.66	15.65

### 6.1. Asphaltenes and nanoaggregates

Calculation of asphaltene precipitation from crude oil requires estimation of a handful of parameters: a) NRTL-SAC conceptual segment numbers for asphaltenes, nanoaggregates, and maltenes, and b) nanoaggregate formation constant,  $K_l^{agg}$ . Since only peripheral alkyl chains of asphaltene molecules in nanoaggregates actively interact with the solvent molecules, the resultant alkyl side chain – solvent interaction can be represented with a proxy *n*-alkane molecule with proper length. Thus, the length or the carbon number of *n*-alkane is another parameter to be estimated.

Estimation of NRTL-SAC conceptual segment parameters requires VLE, LLE, and/or SLE data. Details of this estimation procedure has been reported in our prior work [25]. Briefly, this work uses the experimental asphaltene precipitation data in 15 binary

**Table 9**  
NRTL-SAC conceptual segments.

	X	Y <sup>-</sup>	Y <sup>+</sup>	Z
Asphaltenes	5.76	1.76	0.76	0
Nanoaggregates	3.00	0	0	0
Maltenes				
Athabasca	1.33	0	1.75	0
Peace River	0.99	0	1.45	0
Cold Lake	1.13	0	1.57	0
<i>n</i> -alkanes [25]				
<i>n</i> -C <sub>5</sub>	0.900	0	0	0
<i>n</i> -C <sub>6</sub>	1.000	0	0	0
<i>n</i> -C <sub>7</sub>	1.133	0	0	0
<i>n</i> -C <sub>8</sub>	1.186	0	0	0
<i>n</i> -C <sub>10</sub>	1.271	0	0	0

solvents [4] reported in Table 1 to determine the conceptual segment parameters for asphaltenes and nanoaggregates. The current formulation of asphaltene fraction contains molecules from aromatics, thiophenes, and quinolines. The chemical structure of molecules of these classes indicate absence of hydrophilic function groups. Thus, the hydrophilic conceptual segment number, Z, is set zero for asphaltenes. The exclusively hydrophobic nature of *n*-alkane sets all the conceptual segment numbers of nanoaggregates except X to zero. The estimated conceptual segment numbers of asphaltenes and nanoaggregates are presented in Table 9. *n*-C<sub>56</sub> is found to be a reasonable proxy molecule for the nanoaggregates as it returns correct experimental asphaltene solubility trend in *n*-alkane solvents, i.e., increase of asphaltene solubility with the increase *n*-alkane carbon number [36]. The molecular structural parameters,  $r_l$  and  $q_l$ , for the nanoaggregates are calculated as 38.2 and 30.9, respectively. The logarithm of nanoaggregate formation constant is estimated as –6.30.

### 6.2. Maltenes

Determination of conceptual segment numbers for maltenes is the last piece of the puzzle in calculating asphaltene precipitation from crude oils. As determined from the molecular characterization, the maltenes fraction of the crude oil contains molecules from paraffins, naphthenes, aromatics, thiophenes, and quinolines. Based on the chemical structures of maltene molecules, maltenes are hydrophobic and polar in nature. Therefore, maltenes are assumed to contain hydrophobic and polar repulsive segments, i.e., X and Y<sup>+</sup>, respectively.

The exact values of the maltenes' conceptual segment numbers, i.e., X and Y<sup>+</sup>, are determined from the experimental precipitation trend upon blending the crude oils with *n*-heptane. See Table 2. Fig. 6 presents the flowchart to estimate the model parameters for maltenes. The conceptual segments of maltenes and nanoaggregate formation constant are iterated until the following objective function,  $F_{min}$ , reaches a minimum value.

$$F_{min} = \sum_i^m \left[ \ln \left( \frac{\hat{x}_i}{x_i} \right) \right]^2 \quad (13)$$

here  $\hat{x}_i$  and  $x_i$  are the calculated and the measured asphaltene solubility respectively in a mixture of heavy oil and *n*-heptane of known volume ratio.  $m$  represents the total number of data points.

Fig. 7 reports experimental asphaltene precipitation by blending *n*-heptane with crude oils Athabasca [8], Peace River [8], and Cold Lake [5,7]. Experimental data are presented as mass ratio of precipitated asphaltene over total crude oil, i.e., asphaltene precipitation yield, at different mass fraction of *n*-heptane. During the

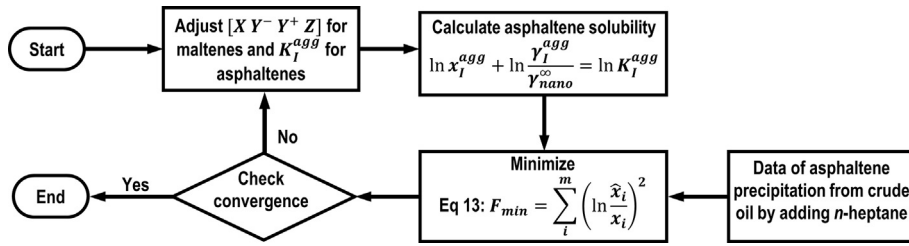


Fig. 6. Flowchart to estimate the conceptual segment numbers for maltenes.

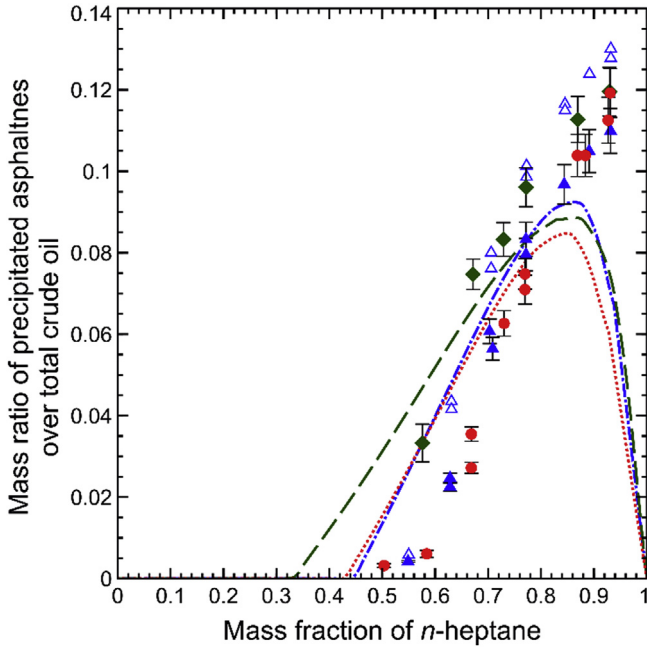


Fig. 7. Asphaltene precipitation yields upon blending with *n*-C<sub>7</sub>. Athabasca [8] (red), Peace River [8] (green), and Cold Lake [5,7] (blue). Symbols and lines are the experimental and predicted precipitations, respectively. Solid symbols are data points used in the regression.

blending process, the average  $Y^+$  conceptual segment number of the blend decreases with the addition of *n*-heptane. As suggested in Fig. 7, asphaltene precipitation happens as the solubility in the mixture decreases. Matching against the precipitation data, the conceptual segments of maltenes are regressed and reported in Table 9. The  $\ln K_I^{agg}$ 's are calculated as  $-3.51$ ,  $-4.04$ , and  $-3.71$  for Athabasca, Peace River, and Cold Lake, respectively. The model successfully captures the asphaltene precipitation behavior including the maximum precipitation yields, as the crude oils are diluted with *n*-heptane. Note that, after reaching the maximum precipitation yields, both the asphaltene contents in the blends of crude oil and *n*-heptane and the asphaltene precipitation yields should drop to zero since the crude oil contents drop to zero when the *n*-heptane mass fractions reach unity. That explains why the model predicts the maximum precipitation yields and the subsequent fall of precipitation yields. The mean absolute deviations (MADs) of model results for asphaltene precipitation yields are further evaluated. See Eq. (14). The overall MADs for Athabasca, Peace River, and Cold Lake are 0.023, 0.020, and 0.066, respectively. The model performs similarly for all three crude oils.

$$MAD = \frac{\sum_i^n |\hat{Y} - Y|}{n} \quad (14)$$

here  $\hat{Y}$  and  $Y$  are calculated and measured asphaltene precipitation yields, respectively, and  $n$  is the number of measurements.

Note that the aggregation formation constant for asphaltenes,  $K_I^{agg}$ , estimated from the precipitation measurements in binary solvents is lower than the corresponding values calculated from the precipitation data from blending of crude oils with *n*-heptane. The asphaltenes used in the precipitation experiments with binary solvents were extracted by diluting the crude oil with high volume ratio, i.e., 40:1, of *n*-heptane and crude oil [4]. Whereas, the asphaltene precipitation measurements from blending crude oils with *n*-heptane were conducted at varying volume ratio of *n*-heptane and crude oil [5,7,8] with the maximum volume ratio of *n*-heptane to crude oil of 20:1. Therefore, the extracted asphaltenes from the two experiments are different and, thus, resulting in different aggregation formation constants.

The stability of asphaltenes in crude oils depends on the solvent power of the maltenes. Higher the aromatic fraction in the maltenes, higher is the asphaltene stability. Despite high asphaltene content in heavy oils, aromatic hydrocarbons in maltenes prevent asphaltenes from precipitation. The reduction of the aromatic content in maltenes, e.g., upon blending with paraffinic hydrocarbons, shifts the asphaltene stability towards precipitation. This blending of crude oils with paraffinic hydrocarbons alters the conceptual segment numbers of maltenes. Fig. 8 shows the effect of conceptual segment numbers of maltenes on asphaltene solubility

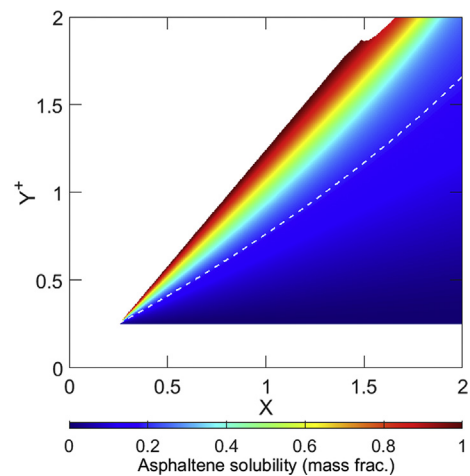


Fig. 8. Dependence of asphaltene solubility with the conceptual segment numbers of maltenes in Athabasca bitumen sample. Dashed line represents the solubility value of 18.96 wt%.

for Athabasca bitumen. The asphaltene solubility increases with the polar repulsive segment number,  $Y^+$ , and decreases with the hydrophobic segment numbers,  $X$ . The dashed line represents the solubility of 18.96 wt%, equivalent to the calculated asphaltene content in Athabasca bitumen. The asphaltenes are stable in the crude oil above this dashed line.

### 6.3. Blends of crude oils and hydrocarbon diluents

With the model parameters identified, asphaltene precipitation behavior can be predicted upon blending the crude oils with hydrocarbon diluents. Conceptual segment numbers for a handful of  $n$ -alkanes were published in the literature [25]. See Table 9. Since  $n$ -alkanes contain only hydrophobic conceptual segment, i.e.,  $X$ , this work takes advantage of published data to develop a linear relationship of  $X$  with  $n$ -alkane carbon number (CN). See Eq. (15).

$$X_{CN} = 0.109CN + 0.354 \quad (15)$$

Fig. 9 shows the predicted volume fractions of normal alkanes required to reach the thermodynamic onset of asphaltene precipitation for Athabasca and Cold Lake bitumen [28], with the alkane carbon number changing from 5 to 16. Interestingly, the required alkane volume fraction increases with the carbon number first till the number reaches 9 then the volume fraction decreases. Known as the paradox of asphaltene precipitation, this trend (solid lines) is well predicted by the model. The MAD values for the model results turn out to be 0.138 and 0.101 for Athabasca and Cold Lake, respectively. As the model calculates the thermodynamic onset of the precipitation, it under-predicts the observed alkane volume fractions required to reach the onset points. When the onset of precipitation is detected by visual observation, one would expect the asphaltenes are already oversaturated in the crude oil –  $n$ -alkane mixtures. The change in Gibbs free energy,  $\Delta G_{M \rightarrow A} / RT$ , and

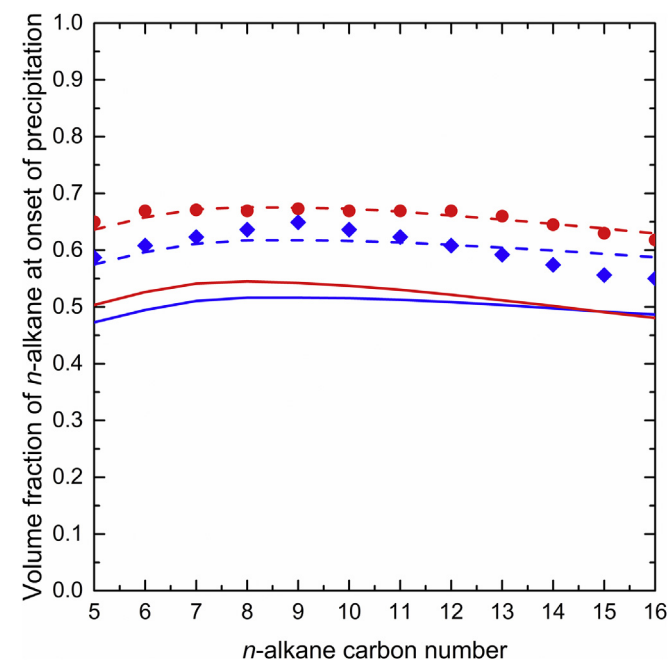


Fig. 9. Volume fraction of  $n$ -alkane at the onset of precipitation: Athabasca [28] (red) and Cold Lake [28] (blue). Symbols and lines are the experimental and predicted results, respectively. The solid lines are generated from the  $\ln K_1^{agg}$ 's estimated from the asphaltene precipitation data. The dashed lines are generated from the  $\ln K_1^{agg}$ 's estimated from the precipitation onset point data.

the corresponding  $\ln K_1^{agg}$  can be calculated from the compositions of multicomponent mixture, i.e., asphaltenes, maltenes, and  $n$ -alkane, at the onset point. The calculated  $\ln K_1^{agg}$  values are nearly constant and, as expected, slightly larger than the values calculated from the precipitation data:  $-3.33 \pm 0.01$  and  $-3.56 \pm 0.04$  for Athabasca and Cold Lake, respectively. Fig. 9 reports the volume fraction of  $n$ -alkane required for the onset of asphaltene precipitation calculated with the observed  $\ln K_1^{agg}$  (dashed lines). The model results match the onset of asphaltene precipitation very well with the MAD values as 0.006 and 0.019 for Athabasca and Cold Lake, respectively.

## 7. Conclusion

This work shows how asphaltene precipitation in crude oils and blends of crude oils with hydrocarbon diluents can be described with the aggregation thermodynamics inspired by the Yen-Mullins model. The crude oils are first expressed in terms of model hydrocarbon molecules and their compositions based on a molecule-based characterization technique and available crude oil assay data. Structures and contents of asphaltenes and maltenes in crude oils are then identified from these model hydrocarbon molecules and their compositions. A total of eight model parameters are further designed to fully characterize asphaltene precipitation in crude oils: two NRTL-SAC conceptual segments for maltenes, three NRTL-SAC conceptual segments for asphaltenes, one NRTL-SAC conceptual segment for nanoaggregates, the carbon number of  $n$ -alkane molecule for the proxy nanoaggregates, and the nanoaggregate formation constant. Combining the molecular characterization technique for petroleum fluids and the NRTL-SAC thermodynamic model for liquid nonideality of complex mixtures, this work extends the applicability of aggregation thermodynamics beyond asphaltene precipitation in pure and binary solvents. It illustrates the utility of aggregation thermodynamics for asphaltene precipitation in crude oils and blends of crude oils with hydrocarbon diluents.

### Declaration of competing interest

The authors declare that they have no known competing financial interests or personal relationships that could have appeared to influence the work reported in this paper.

### CRediT authorship contribution statement

**Md Rashedul Islam:** Methodology, Software, Validation, Formal analysis, Investigation, Data curation, Writing - original draft, Visualization. **Yifan Hao:** Software, Validation, Formal analysis, Investigation, Data curation, Writing - original draft. **Chau-Chyun Chen:** Conceptualization, Validation, Resources, Writing - review & editing, Supervision, Project administration, Funding acquisition.

### Acknowledgements

The authors gratefully acknowledge the financial support of the Jack Maddox Distinguished Engineering Chair Professorship in Sustainable Energy sponsored by the J.F Maddox Foundation.

### References

- [1] R. Cimino, S. Corraera, A. Del Bianco, T.P. Lockhart, Solubility and phase behavior of asphaltenes in hydrocarbon media, in: E.Y. Sheu, O.C. Mullins (Eds.), *Asphaltenes: Fundamentals and Applications*, Plenum Press, New York, 1995, pp. 97–130.
- [2] A. Hirschberg, L. DeJong, B. Schipper, J. Meijer, Influence of temperature and pressure on asphaltene flocculation, *Soc. Petrol. Eng. J.* 24 (3) (1984) 283–293.

- [3] H.W. Yarranton, J.H. Masliyah, Molar mass distribution and solubility modeling of asphaltenes, *AIChE J.* 42 (12) (1996) 3533–3543.
- [4] K.D. Mannistu, H.W. Yarranton, J.H. Masliyah, Solubility modeling of asphaltenes in organic solvents, *Energy Fuel.* 11 (3) (1997) 615–622.
- [5] H. Alboudwarej, K. Akbarzadeh, J. Beck, W.Y. Svrcek, H.W. Yarranton, Regular solution model for asphaltene precipitation from bitumens and solvents, *AIChE J.* 49 (11) (2003) 2948–2956.
- [6] K. Akbarzadeh, A. Dhillon, W.Y. Svrcek, H.W. Yarranton, Methodology for the characterization and modeling of asphaltene precipitation from heavy oils diluted with *n*-alkanes, *Energy Fuel.* 18 (5) (2004) 1434–1441.
- [7] K. Akbarzadeh, H. Alboudwarej, W.Y. Svrcek, H.W. Yarranton, A generalized regular solution model for asphaltene precipitation from *n*-alkane diluted heavy oils and bitumens, *Fluid Phase Equil.* 232 (1–2) (2005) 159–170.
- [8] A.K. Tharanivasan, W.Y. Svrcek, H.W. Yarranton, S.D. Taylor, D. Merino-Garcia, P.M. Rahimi, Measurement and modeling of asphaltene precipitation from crude oil blends, *Energy Fuel.* 23 (8) (2009) 3971–3980.
- [9] D.E. Freed, O.C. Mullins, J.Y. Zuo, Theoretical treatment of asphaltene gradients in the presence of GOR gradients, *Energy Fuel.* 24 (7) (2010) 3942–3949.
- [10] J.Y. Zuo, O.C. Mullins, D. Freed, H. Elshahawi, C. Dong, D.J. Seifert, Advances in the Flory–Huggins–Zuo equation of state for asphaltene gradients and formation evaluation, *Energy Fuel.* 27 (4) (2013) 1722–1735.
- [11] J. Wu, J.M. Prausnitz, A. Firoozabadi, Molecular-thermodynamic framework for asphaltene-oil Equilibria, *AIChE J.* 44 (5) (1998) 1188–1199.
- [12] D.L. Gonzalez, G.J. Hirasaki, J. Creek, W.G. Chapman, Modeling of asphaltene precipitation due to changes in composition using the perturbed chain statistical associating fluid theory equation of state, *Energy Fuel.* 21 (3) (2007) 1231–1242.
- [13] F.M. Vargas, D.L. Gonzalez, G.J. Hirasaki, W.G. Chapman, Modeling asphaltene phase behavior in crude oil systems using the perturbed chain form of the statistical associating fluid theory (PC-SAFT) equation of state, *Energy Fuel.* 23 (3) (2009) 1140–1146.
- [14] O.C. Mullins, The modified yen model, *Energy Fuel.* 24 (4) (2010) 2179–2207.
- [15] B. Schuler, G. Meyer, D. Peña, O.C. Mullins, L. Gross, Unraveling the molecular structures of asphaltenes by atomic force microscopy, *J. Am. Chem. Soc.* 137 (31) (2015) 9870–9876.
- [16] B. Schuler, S. Fatayer, G. Meyer, E. Rogel, M. Moir, Y. Zhang, M.R. Harper, A.E. Pomerantz, K.D. Bake, M. Witt, D. Peña, J.D. Kushnerick, O.C. Mullins, C. Ovalles, F.G.A. van den Berg, L. Gross, Heavy oil based mixtures of different origins and treatments studied by atomic force microscopy, *Energy Fuel.* 31 (7) (2017) 6856–6861.
- [17] B. Schuler, Y. Zhang, S. Collazos, S. Fatayer, G. Meyer, D. Pérez, E. Guitián, M.R. Harper, J.D. Kushnerick, D. Peña, L. Gross, Characterizing aliphatic moieties in hydrocarbons with atomic force microscopy, *Chem. Sci.* 8 (3) (2017) 2315–2320.
- [18] M. Wang, Y. Hao, M.R. Islam, C.-C. Chen, Aggregation thermodynamics for asphaltene precipitation, *AIChE J.* 62 (4) (2016) 1254–1264.
- [19] Chen, C. C.; Hao, Y.; Wang, M.; Islam, M. R. Apparatus and Computerized Method for Predicting Asphaltene Precipitation Based on Aggregation Thermodynamics. US Patent Application No. 20180314806 A1, Nov. 01, 2018.
- [20] A. Fredenslund, R.L. Jones, J.M. Prausnitz, Group-contribution estimation of activity coefficients in nonideal liquid mixtures, *AIChE J.* 21 (6) (1975) 1086–1099.
- [21] M.R. Islam, Y. Hao, M. Wang, C.-C. Chen, Prediction of asphaltene precipitation in organic solvents via COSMO-SAC, *Energy Fuel.* 31 (9) (2017) 8985–8996.
- [22] M.R. Islam, C.-C. Chen, COSMO-SAC sigma profile generation with conceptual segment concept, *Ind. Eng. Chem. Res.* 54 (16) (2015) 4441–4454.
- [23] Chen, C. C.; Islam, M. R. Apparatus and Computerized Method for Optimizing or Generating a Sigma Profile for a Molecule. US Patent Application No. 20170083688 A1, Mar. 23, 2017.
- [24] S.T. Lin, S.I. Sandler, A priori phase equilibrium prediction from a segment contribution solvation model, *Ind. Eng. Chem. Res.* 41 (5) (2002) 899–913.
- [25] M.R. Islam, Y. Hao, C.-C. Chen, Thermodynamic modeling of asphaltene precipitation in pure and mixed solvents with NRTL-SAC, *Fluid Phase Equil.* 473 (2018) 255–261.
- [26] C.-C. Chen, Y. Song, Solubility modeling with a nonrandom two-liquid segment activity coefficient model, *Ind. Eng. Chem. Res.* 43 (26) (2004) 8354–8362.
- [27] Chen, C.-C.; Que, H. L. Method of Characterizing Chemical Composition of Crude Oil for Petroleum Processing. U.S. Patent No. 9,934,367 B2, Apr. 03 2018.
- [28] I.A. Wiehe, H.W. Yarranton, K. Akbarzadeh, P.M. Rahimi, A. Teclemariam, The paradox of asphaltene precipitation with normal paraffins, *Energy Fuel.* 19 (4) (2005) 1261–1267.
- [29] G. Hotier, M. Robin, Action de Divers Diluants sur les Produits Pétroliers Lourds: mesure, Interprétation et Prédiction de la Floculation des Asphaltènes, *Rev. Inst. Fr. Petrol* 38 (1) (1983) 101–120.
- [30] D.S. Abrams, J.M. Prausnitz, Statistical thermodynamics of liquid mixtures: a new expression for the excess Gibbs energy of partly or completely miscible systems, *AIChE J.* 21 (1) (1975) 116–128.
- [31] A.A. Bondi, *Physical Properties of Molecular Crystals, Liquids and Glasses*, Wiley, New York, 1968.
- [32] C.-C. Chen, A segment-based local composition model for the Gibbs energy of polymer solutions, *Fluid Phase Equil.* 83 (1993) 301–312.
- [33] J. Gross, G. Sadowski, Perturbed-chain SAFT: an equation of state based on a perturbation theory for chain molecules, *Ind. Eng. Chem. Res.* 40 (4) (2001) 1244–1260.
- [34] Aspen HYSYS®, V 8.4, Aspen Technology Inc., Bedford, MA, 2013.
- [35] Alberta government: bitumen assay program (BAP) aggregate assay information. <https://open.alberta.ca/opendata/bitumen-assay-program-bap-aggregate-assay-information> (accessed Jan. 08, 2020).
- [36] D.L. Mitchell, J.G. Speight, The solubility of asphaltenes in hydrocarbon solvents, *Fuel* 52 (2) (1973) 149–152.